Phase Behavior and Interactions of the Membrane-Protein Bacteriorhodopsin

I. Koltover,[1] J. O. Raedler,[1] T. Salditt,[1] K. J. Rothschild,[2] and C. R. Safinya[1]
[1]*Materials Department, Physics Department, and Biochemistry and Molecular Biology Program, University of California, Santa Barbara, California 93106*
[2]*Department of Physics and Molecular Biophysics Laboratory, Boston University, Boston, Massachusetts 02215*
(Received 29 September 1998)

We present a synchrotron x-ray diffraction study of melting in stacks of two-dimensional crystalline arrays of the membrane protein bacteriorhodopsin. Two distinct regimes have been found as a function of the intermembrane distance d. In the "coupled" regime for $d < 250$ Å the temperature (T_m) of the melting transition decreases with increasing d, demonstrating the effect of the repulsive membrane interactions on the intramembrane protein ordering. For $d > 250$ Å a "decoupled" regime is found with higher T_m^* independent of d. Below T_m^* a solid-liquid-solid reentrant behavior is observed as d is increased. [S0031-9007(99)08795-5]

PACS numbers: 87.15.By, 61.30.Eb, 64.70.Md, 87.22.Bt

Integral membrane proteins play a critical role in many cell functions, such as selective molecular transport across the membrane, energy transduction, and response to extracellular stimuli. Their interaction within the membrane may lead to ordered arrays, which can affect the elasticity and conformation of their host membranes [1]. Little is known about these interactions and the physical nature of the membrane protein self-assemblies, in contrast to pure lipid membranes, which have been intensively studied [2]. These self-assemblies can affect the temperature stability of their membrane proteins and may be utilized in protein-based biotechnological applications [3,4].

In biological systems the electrostatic, van der Waals, and hydration intermembrane interactions can affect the behavior of the membrane protein self-assembly. More generally, the ordered protein arrays within their host membranes are models of two-dimensional (2D) crystals embedded in three-dimensional space. Compared to a simple 2D solid, these systems are more complex and have additional internal degrees of freedom due to the protein secondary structures and the membrane lipid matrix.

In this Letter, we report a synchrotron x-ray diffraction study in aligned multilayers of charged membranes containing ordered hexagonal arrays of the membrane protein bacteriorhodopsin (bR) [Fig. 1(a)]. These arrays undergo a melting order-disorder transition as a function of increasing temperature [4,5] and have no interlayer positional correlations. Thus, they correspond to a model of untethered 2D solid membranes embedded in three dimensions. We have measured the strength of the protein interactions and investigated the mechanism of the protein 2D crystal melting transition. The ability to swell the multilayer stack with water further allowed us to tune the strength of the intermembrane interactions and study their effect on the protein correlations and order within the membrane, thus obtaining, for the first time, a comprehensive phase diagram of the membrane protein self-assembly.

bR is found in the purple membrane (PM) of the bacterium *Halobacterium salinarium* cells. It is a light driven proton pump and can be purified in the form of membrane patches of ~0.5 μm size and 47 Å thickness. The protein molecules consist of seven transmembrane α helices and are organized into 44 Å diameter trimers which form a regular hexagonal lattice in the plane of the membrane [Fig. 1(a), right] [6]. The protein trimers constitute ~75% of PM by weight, with the rest comprised of lipids with fluid hydrocarbon chains. PM is overall negatively charged, which leads to stacks of mutually repelling membranes which can be swollen with water by controlling the surrounding vapor pressure, thereby changing the multilayer periodicity d [Fig. 1(a), left].

bR multilayers were prepared from purified suspensions of the native 0.5 μm diameter PM's which were extensively washed with deionized water to ensure negligible

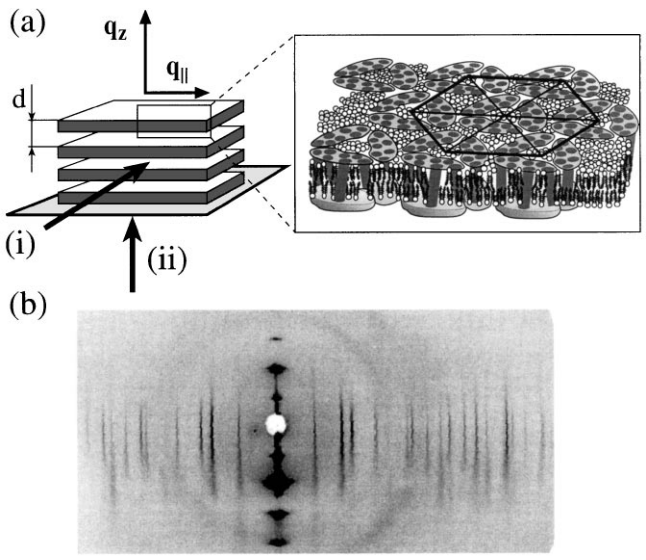

FIG. 1. (a) Schematic of the bR multilayer and the experimental x-ray diffraction geometry. (b) Rectangular section of the 2D diffraction image of the bR multilayer in the reflection (ii) geometry.

 0031-9007/99/82(15)/3184(4)$15.00

solution ionic strength. Thick (~ 10 μm) multilayers were made on the hydrophilic surface of polished ultrathin (25 μm) Si wafers (Virginia Semiconductor) and placed in an environmental chamber with x-ray transparent windows. To control independently the sample relative humidity (RH) and temperature, the chamber had a water reservoir kept at a temperature lower than the sample. The temperature stability was ± 0.005 K over a period of several hours and uniformity < 0.05 K over the sample area (1 cm^2). Rising the RH increased the amount of water in the sample and set the water chemical potential in the multilayer. Synchrotron x-ray experiments were done at Stanford Synchrotron Radiation Laboratory (SSRL) using a small angle diffraction setup with an image plate area detector (MAR Research) at a distance 0.6 m from the sample. A 200 μm $\times$ 200 μm x-ray beam was defined with slits, giving a symmetric resolution of 0.0015 Å^{-1}.

Two x-ray diffraction geometries were used [Fig. 1(a), left]: (i) transmission, with the x-ray beam incident normal to the sample surface, and (ii) reflection, with the beam parallel to the sample. An example of the x-ray diffraction image of a bR multilayer at low humidity and room temperature (25 °C) in the reflection geometry is shown in Fig. 1(b). The sharp reflections along the vertical q_z axis are due to the periodicity $d = 54$ Å of the multilayer stack. They appear as arcs because of the finite mosaic spread of the individual PM orientations with a mosaicity of 6°. The vertically elongated spots (Bragg cylinders) along the horizontal $q_\parallel$ direction are the reflections of the hexagonal lattice of protein trimers with a unit cell spacing $a = 63.4$ Å. They extend along q_z, indicating that the protein 2D crystals have no positional correlations between the neighboring membrane layers, which would result in a sharp modulation of the intensity along the rods [7]. The limited length of these reflections is due to the finite thickness of the proteins and their intensity along q_z is modulated by the protein form factor.

In the transmission geometry, the protein lattice reflections appear as a set of concentric rings because the large x-ray beam (0.2 mm^2) illuminated many single protein crystals (0.5 μm^2). Thus, we were not directly experimentally sensitive to the possible orientational correlations of the adjacent protein lattices. The azimuthally averaged intensity distributions as a function of temperature at two different multilayer hydration levels are presented in Figs. 2(a) and 2(b). At low temperature, we observe many orders of sharp reflections, indicating that the protein 2D crystal is well ordered. As the temperature is increased, the ordered lattice melts into a well-correlated protein 2D liquid (top scans), with the correlation length $\xi = 149$ Å ~ 2 coordination shells resulting in the observation of multiple orders of liquid diffraction peaks. The scans in Figs. 2(a) and 2(b) at temperatures slightly below melting show coexistence between the protein lattice and the protein liquid. Thus, the melting transition of the bR 2D crystals is first order at all of the studied separations d between the membranes. While both controlled experimental parameters (T, d) are external fields, we observed a broad 2D solid-liquid coexistence regime because of the finite PM area fixed the protein concentration, rather than chemical potential in the membrane.

To gain insight into the mechanism of melting, we recall that the 2D crystals are unstable against long-wavelength thermal vibrations. They posses only quasi-long-range order with positional correlations decaying algebraically to zero at large distances $\langle [\rho_{\mathbf{G}(hk)}(\mathbf{R}) - \rho_{-\mathbf{G}(hk)}(0)]^2 \rangle \propto e^{i\mathbf{G}(hk)\cdot\mathbf{R}} R^{-\eta_{\mathbf{G}(hk)}}$, where $\mathbf{G}(hk)$ is a reciprocal lattice vector of the 2D crystal. This results in the power law singularities in the position of the Bragg peaks, rather than the δ-function-like reflections of long-range-ordered 3D crystals. This can be seen in Fig. 2(c) displaying the (11) and (20) peaks of the protein crystal at $d = 190.3$ Å and $T = 45.2$ °C, which are broader and have intense thermal diffuse scattering (TDS) tails compared to the experiment resolution function (dashed line). The asymmetric shape of the Bragg peaks is a characteristic signature of 2D crystals, resulting from the finite length of the rods and sample mosaicity [7,8].

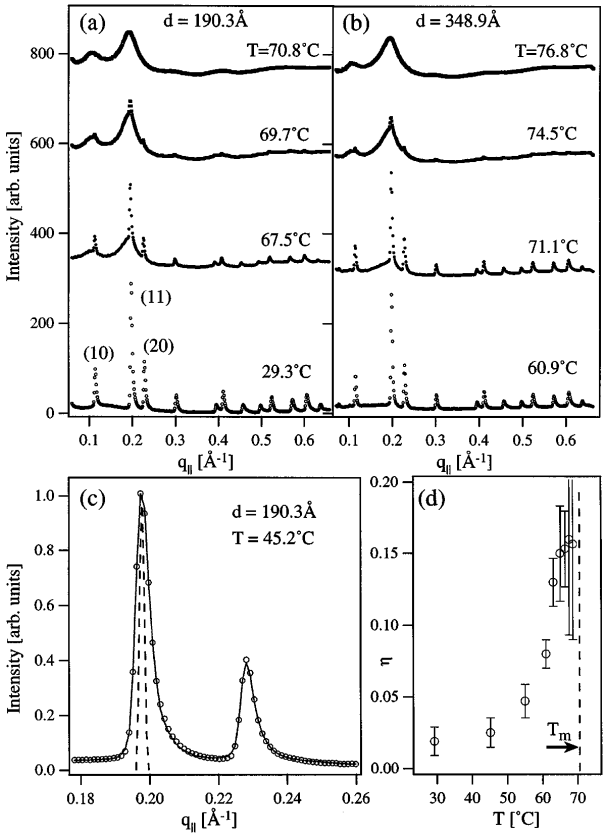

FIG. 2. (a),(b) x-ray scans as a function of temperature of the bR multilayers at $d = 190.3$ Å (a) and $d = 348.9$ Å (b); (c) (11) and (20) peaks of the x-ray scan of bR hexagonal lattice at $d = 190.3$ Å and $T = 45.2$ °C. Solid line is the fit of the 2D harmonic hexagonal lattice model structure factor. Dashed line is the experimental resolution function; (d) $\eta = \eta_{(10)}(T)$ values obtained from fitting protein peaks at $d = 190.3$ Å.

The structure factor of a harmonic 2D crystal with finite domain size L has been derived analytically and is known to describe 2D physisorbed rare gases [7,8]. It has a power law form asymptotically close to each reciprocal lattice vector

$$S(\mathbf{q}_\parallel, \mathbf{G}(hk)) \propto 1/[\mathbf{q}_\parallel - \mathbf{G}(hk)]^{(2-\eta_{\mathbf{G}(hk)})}, \quad (1)$$

with Gaussian central part of width $\sim I/L$. The exponent η is related to the Lamé elastic coefficients μ and λ of the 2D harmonic lattice [4,8],

$$\eta_{\mathbf{G}(hk)} = c k_B T \mathbf{G}^2(hk)/4\pi\mu,$$
$$\text{with } 1 < c \equiv (3 + \lambda/\mu)/(2 + \lambda/\mu) < 2, \quad (2)$$

where the prefactor c is limited due to the thermodynamic stability constraints on the compressibility modulus $(\lambda + \mu) > 0$ and the shear modulus $\mu > 0$. Thus, the line shape of the 2D protein crystal peaks allows a determination of the domain size L as well as an estimate (within a factor of 2) of the shear modulus μ. The former measures the degree of crystal perfection, while the latter gauges the strength of the protein interactions.

The fit of the 2D harmonic crystal model line shape to the data at $T = 45.2\,^\circ$C is shown as the solid line in Fig. 2(c) [9] and is remarkably good, considering that the experimental system consists of huge protein trimers in a very high density membrane which is not necessarily flat. We find $L = 3820 \pm 200$ Å and $\eta = \eta_{(10)} = 0.025 \pm 0.005$. Assuming $\mu = \lambda$ (a reasonable assumption for a triangular lattice) with $c = 4/3$ in (2), we obtain the estimate $\mu a^2 = 230 k_B T$ or $\mu = 20$ dyn/cm. The domain size is roughly equal to the diameter of the PM patches used to prepare the sample. The measured η increases as a function of temperature, approaching $\eta(T_m) = 0.15$ [Fig. 2(d)], but remains nearly independent of T close to and below T_m. Combined with the observed rapid decrease of L near T_m, this suggests that the melting of the bR lattice proceeds by a first order transition with proliferation of the lattice defects, which may be preemptying a continuous melting. The first order nature of the melting is manifested by the large hysteresis in the bR crystal order parameter ($\propto$ inverse of the lattice spacing a) as a function of T [Fig. 3(a)].

Close to room temperature, the measured μ is similar to that usually found in colloidal crystals and is much smaller than the shear moduli of typical solid-state crystals ($\sim 10^{13}$ dyn/cm^2) [10]. Therefore, the protein-protein forces are also of the magnitude close to those in sterically or electrostatically stabilized colloidal crystals. Forces of similar strength are also predicted to result from the membrane deformation mediated interactions between the inclusions (proteins) [11].

It is clear from Figs. 2(a) and 2(b) that, although the neighboring stacked 2D protein crystals are positionally decoupled, the melting transition temperature T_m depends strongly on the membrane separation d: The crystal at $d = 190.3$ Å melts at lower temperature ($T_m = 70.8\,^\circ$C) than the crystal at $d = 348.9$ Å [Fig. 2(b), $T_m = 76.6\,^\circ$C]. The $T_m(d)$ dependence is strikingly manifested by the melting of the protein crystal at constant temperature with increasing d: Fig. 3(b) shows a series of in-house x-ray diffraction scans at $T = 80.3\,^\circ$C where the bR lattice expands and melts with the increasing d at $d_m = 57.1$ Å.

We show in Fig. 4 the phase diagram of the bR 2D crystal stacks. The $T_m(d)$ dependence is nonmonotonic, decreasing for $d < 200$ Å [regime (I)] and increasing for $d > 250$ Å [regime (II)]. The $T_m(d)$ decrease in regime (I) is clearly demonstrated by the constant T melting of Fig. 3(b), while the T_m reentrance of regime (II) is evident from Figs. 2(a) and 2(b), where at $T = 71\,^\circ$C we find liquid at $d = 190.3$ Å and a well ordered crystal at $d = 348.9$ Å. The dramatic difference between the two regimes (I) and (II) indicates that they correspond to two different thermodynamic states of the protein self-assembly. Because the protein crystals have no interlayer positional correlations at all d studied, we conclude that the observed $T_m(d)$ dependence is due to the overall repulsive electrostatic interaction between the membranes or the possible orientational correlations of the protein lattices. In particular, since $T_m = 75.5\,^\circ$C is independent of d in the regime (II), it corresponds to the completely decoupled state of the 2D protein crystals.

From the measured value of η_m, we estimate the amplitude of vibration of the proteins around their average

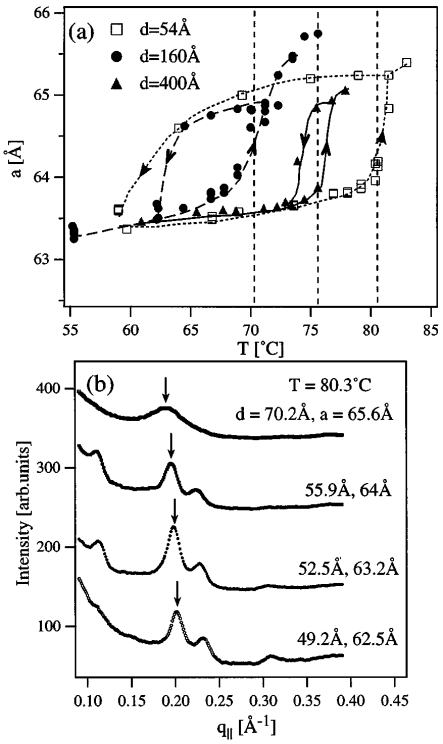

FIG. 3. (a) Hysteresis curves of the order parameter (lattice spacing a) of the 2D protein lattice melting as a function of temperature at three different fixed d. Solid and dashed lines through the data are guides to the eye. Vertical dashed lines indicate the melting temperatures; (b) in-house (lower resolution) x-ray scans showing the melting of bR lattice at constant $T = 80.3\,^\circ$C with increasing multilayer hydration (d).

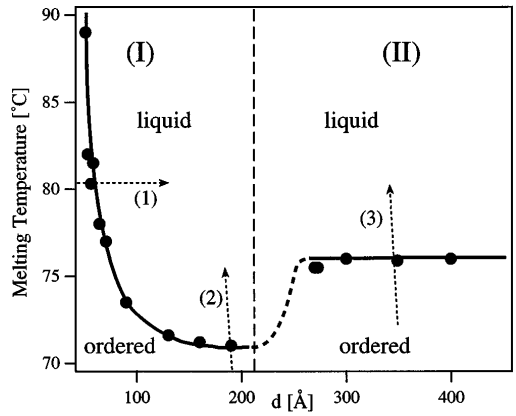

FIG. 4. Phase diagram of the bR multilayers as a function of temperature T and repeat distance d controlled by the amount of water in the sample. Solid line is the solid-liquid $T_m(d)$ phase boundary of the bR protein 2D crystal. Dashed arrows correspond to the paths of data shown in Figs. 3(a) (1), 2(a) (2), and 2(b) (3).

positions in the hexagonal lattice $\sqrt{\langle \Delta u \rangle^2} \approx 3.8$ Å. Thus $\Delta u/a \approx 0.06$ is less than the Lindemann criterion of melting (0.1) and the crystal should be unstable against an overall lattice stretching. Such stretching explains regime (I) of the phase diagram, where the membranes strongly repell electrostatically. We expect the membrane surface area to expand as d increases with increasing hydration in multilayers of mutually repelling membranes [12]. This is what is observed as we show in Fig. 3(b), where the position of the (11) peak shifts to lower q indicating that a increases by $\sim$3 Å. Thus, the protein lattice density decreases as the bR lattice undergoes a melting transition with increasing d at constant $T = 80.3$ °C. Therefore, in regime (I) of the phase diagram the intermembrane repulsion stabilizes the bR lattice with a larger protein density with decreasing d by squeezing it together.

Regime (II) of the phase diagram shows a completely new reentrant behavior of the 2D crystal melting. Here, $T_m = T_m^*$ is independent of d above a critical membrane separation $d_c \sim 250$ Å, corresponding to a completely decoupled state of the 2D protein lattices. In order to explain the reentrant behavior, we propose that the 2D lattices in regime (I) are orientationally correlated between membrane layers. The orientational decoupling of crystals in regime (II) (for $d > d_c$) increases their entropy, which is consistent with the observation of an increase in T_m. A similar reentrant behavior has been observed in the solid-liquid transition of weakly incommensurate phases of 2D noble gas solids physisorbed on periodic substrates [13]. Also, in a related lower dimensional system consisting of 1D lattices of DNA chains absorbed on membranes [14], recent theory predicts the possible existence of a phase with interlayer orientational (but not positional) coupling [15].

An indirect support for this explanation can be obtained by considering the hysteresis curves of the bR crystal order parameter a as a function of T [Fig. 3(a)]. In regime (I) of the phase diagram, the melting is highly hysteretic, as expected in a strongly first order phase transition. The area of the hysteresis loops decreases with increasing d and becomes quite small at $d > 250$ Å. This is because in regime (I) both intralayer positional and interlayer orientational degrees of freedom of a stack melt simultaneously, whereas in the orientationally decoupled regime (II) melting involves only the disappearance of intralayer positional correlations. The melting transition however remains first order.

Further synchrotron x-ray studies of the larger single-crystal samples should allow one to quantitatively investigate the role of defects and orientational membrane coupling in the protein lattice melting transition, as well as the crossover between regimes (I) and (II).

We thank T. Lubensky, L. Golubovic, R. Menes, and P. Pincus for valuable discussions. This work was supported by NSF-DMR-9624091, NSF-DMR-9972246, and Los Alamos National Laboratory-STB/UC:98-202. The Materials Research Laboratory is supported by NSF-DMR-9632716. SSRL is supported by the U.S. DOE.

[1] *Structure and Dynamics of Membranes*, edited by R. Lipowsky and E. Sackmann (Elsevier, New York, 1995).
[2] *Micelles, Membranes, Microemulsions and Monolayers*, edited by W. M. Gelbart, A. Ben-Shaul, and D. Roux (Springer-Verlag, Berlin, 1994).
[3] *Nanofabrication and Biosystems*, edited by H. C. Hoch, L. W. Jelinsky, and H. G. Craighead (Cambridge University, Cambridge, England, 1996).
[4] Y. Shen, C. R. Safinya, K. S. Liang, A. F. Ruppert, and K. J. Rothschild, Nature (London) **366**, 48 (1993); C. R. Safinya and Y. Shen, in *Physics of Biomaterials: Fluctuations, Selfassembly and Evolution*, edited by T. Riste and D. Sherrington (Kluwer, Dordrecht, 1995).
[5] K. Hiraki *et al.*, Biochim. Biophys. Acta **647**, 18 (1981).
[6] R. Henderson *et al.*, J. Mol. Biol. **213**, 899 (1990).
[7] P. A. Heiney *et al.*, Phys. Rev. B **28**, 6416 (1983); P. Dimon *et al.*, Phys. Rev. B **31**, 437 (1985).
[8] D. R. Nelson and B. I. Halperin, Phys. Rev. B **19**, 2456 (1979); P. Dutta and S. K. Sinha, Phys. Rev. Lett. **47**, 50 (1981).
[9] $S(q)$ is averaged over the individual PM mosaicity using a procedure similar to Ref. [8] [I. Koltover and C. R. Safinya (to be published)].
[10] H. M. Lindsay and P. M. Chaikin, J. Phys. (Paris) Colloq. **46**, C3-269 (1985).
[11] N. Dan *et al.*, J. Phys. II (France) **4**, 1713 (1994).
[12] V. A. Parsegian, J. Theor. Biol. **15**, 70 (1967).
[13] S. N. Coppersmith *et al.*, Phys. Rev. B **25**, 349 (1982); H. Hong *et al.*, Phys. Rev. B **40**, 4797 (1989).
[14] J. O. Rädler, I. Koltover, T. Salditt, and C. R. Safinya, Science **275**, 810 (1997); T. Salditt, I. Koltover, J. O. Radler, and C. R. Safinya, Phys. Rev. Lett. **79**, 2582 (1997).
[15] C. S. O'Hern and T. C. Lubensky, Phys. Rev. Lett. **80**, 4345 (1998); L. Golubovic and M. Golubovic, *ibid.* **80**, 4341 (1998).